PUZZLING RESULTS ON NUCLEAR SHELLS FROM THE PROPERTIES OF FISSION CHANNELS

K.-H. SCHMIDT, A.R. JUNGHANS

*Gesellschaft für Schwerionenforschung, Planckstraße 1, 64291 Darmstadt,
Germany*
E-mail: k.h.schmidt@gsi.de

J. BENLLIURE

Universidad de Santiago de Compostela, 15706 Santiago de Compostela, Spain

C. BÖCKSTIEGEL, H.-G. CLERC, A. GREWE, A. HEINZ, M. DE JONG,
S. STEINHÄUSER

*Institut für Kernphysik, TU Darmstadt, Schloßgartenstr. 9, 64289 Darmstadt,
Germany*

At the secondary-beam facility of GSI, the fission properties of short-lived neutron-deficient nuclei have been investigated in inverse kinematics. Detailed features of the measured element distributions and total kinetic energies seem to contradict the present understanding according to which the neutron shells at $N = 82$ and $N \approx 90$ are decisive for the asymmetric fission channels.

1 Introduction

Nuclear fission is one of the most intensively studied types of nuclear reaction[1,2]. All nuclei investigated from about ^{234}U to ^{256}Fm were found to fission into fragments with strongly different mass. Symmetric fission is suppressed. The mean mass of the heavy component is almost stationary. Obviously, shell effects in the heavy fragment control this asymmetric fission. The most important shells are considered to be the spherical $N = 82$ shell and a shell at $N \approx 90$ at large deformation ($\beta \approx 0.6$)[3].

But asymmetric fission dies out on both extremes of the mass range. There is a dramatic change of the mass distribution to a narrow single-humped distribution found in ^{258}Fm[4]. This is explained by the formation of two spherical nuclei close to the doubly magic ^{132}Sn. Selected nuclei in this range are accessible to experiment because they decay by spontaneous fission. But also for lighter nuclides one observes single-humped distributions, e.g. for ^{213}Ac. However, these are much broader. The present work reports on the first systematic study of the transition form asymmetric to symmetric fission below ^{234}U. Previously, only a few mass distributions from low excitation energies could be measured by use of radioactive targets ^{226}Ra and ^{227}Ac (see

e.g.[5]). Some other nuclei in the suspected transition region between ^{225}Ac and ^{213}At had been produced with excitation energies around 30 MeV by fusion reactions[6,7,8].

2   The Secondary-beam Experiment

In a conventional fission experiment, a target nucleus is excited. The fission fragments reach the detectors with a kinetic energy given by the fission process. The available target materials limit the experiments on low-energy fission. Up to now, spontaneous fission offers the only possibility to overcome this limitation for those nuclei of interest which can be produced e.g. by heavy-ion fusion reactions.

The secondary-beam facility of GSI allows now becoming independent of available target nuclides. By fragmentation of a ^{238}U beam at 1 A GeV, many short-lived radioactive nuclei are produced. After isotopic separation in the fragment separator, several hundred fissile nuclei are available for nuclear-fission studies[9,10,11]. In the present experiment, fission was induced by Coulomb excitation of the secondary beam in a lead-target. The atomic numbers and the velocity vectors of both fission fragments were determined, and the element distributions and the mean total kinetic energies were deduced. The experimental technique is described in detail in Ref.[12].

The electromagnetic field of a lead target nucleus as seen by the secondary projectiles can be formulated as a flux of equivalent photons according to Ref.[13]. At relativistic energies as employed here, the spectrum is hard enough to excite giant resonances in the secondary projectiles. With the calculated equivalent photon spectrum and the systematics of the photo-absorption cross sections, one can calculate the energy-differential cross section for electromagnetic excitation. It peaks at about 11 MeV and is very similar for all nuclides investigated.

3   Results and Discussion

The data acquired in the secondary-beam experiment allow for the first time to systematically analyse the fission properties of nuclei in a large continuously covered region on the chart of the nuclides. Fig. 1 shows the elemental yields after electromagnetic-induced fission, covering the transition from a single-humped element distribution at ^{221}Ac to a double-humped element distribution at ^{234}U. In the transitional region, around ^{227}Th, triple-humped distributions appear, demonstrating comparable weights for asymmetric and symmetric fission.
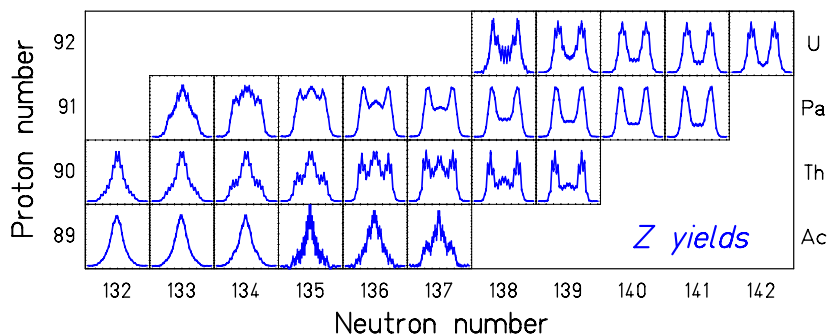
Figure 1. Measured fission-fragment element distributions in the range $Z = 24$ to $Z = 65$ after electromagnetic excitation of 28 secondary beams between ^{221}Ac and ^{234}U are shown on a chart of the nuclides.

The transition seems to be governed by the mass number of the fissioning system as the ordering parameter: Systems with constant mass show similar charge distributions.

Another important parameter deduced from the data is the mean position of the heavy fission-fragment component shown in Fig. 2. From previously measured mass distributions, a roughly constant position of the heavy fission component in mass number had been deduced [14]. Due to the long isotopic chains investigated and the high precision of the data, we obtain a much more comprehensive view. It becomes very clear that the position of the heavy component is almost constant in atomic number $Z \approx 54$ and moves considerably in neutron number. This also means that the position accordingly moves in mass number. It is not expected that any polarisation in N/Z which is neglected here due to the UCD (unchanged charge density) assumption can explain the observed variation of five units in neutron number from $N = 79$ to $N = 84$.

Both findings, the mass as the ordering parameter of the transition and the constant position at $Z = 54$ are unexpected, since the asymmetric fission component is usually traced back to the influence of neutron shells in the heavy component (e. g.[3]).

According to the present understanding of the fission process, the different components which appear in the yields and in the kinetic-energy distributions of the fission fragments are attributed to fission channels[15,16,17,18] which are assigned to valleys in the potential-energy surface of the highly deformed sys-
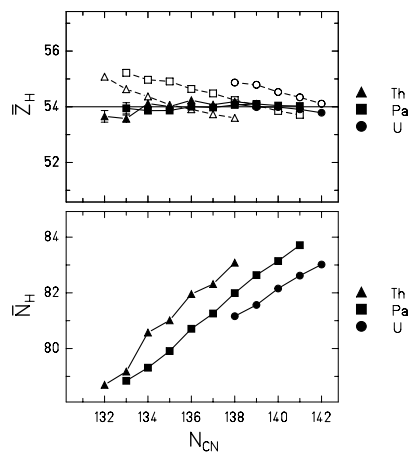
Figure 2. Full symbols: Measured mean position of the heavy asymmetric component in nuclear-charge number Z_H (upper part) and neutron number N_H (lower part). While the charge number was measured, the neutron number was estimated by the UCD assumption: $N_H = Z_H * N_{CN}/Z_{CN}$. Open symbols: Result of the model calculation described in the text.

tem due to shell effects. Since it is not well understood, how the yields of the different fission channels are determined in the dynamic evolution of the fissioning system, it has become a standard to determine the parameters of the fission channels from a fit to the data by assuming that each of the independent fission channels is characterised by a Gaussian-like peak in the mass or element distribution and a specific elongation of the scission configuration which determines the total kinetic energy.

Figure 3 shows the result of a fit to six selected systems, covering the transition from asymmetric fission to symmetric fission. Obviously, the measured data can well be represented by the superposition of the three independent fission channels which also appear in heavier systems. However, we observe two remarkable features. Firstly, the positions of both asymmetric fission channels appear to be astonishingly constant in proton number at $Z = 53$ and $Z = 55$, respectively, although the neutron number of the fissioning system varies. Secondly, the kinetic energy of the super-long fission channel approaches that of the standard II channel for the lightest systems. This shows that the scission-point configuration of the super-long channel becomes more compact with decreasing mass number of the fissioning nucleus. This is a sign for the influence of shell effects also in symmetric fission.

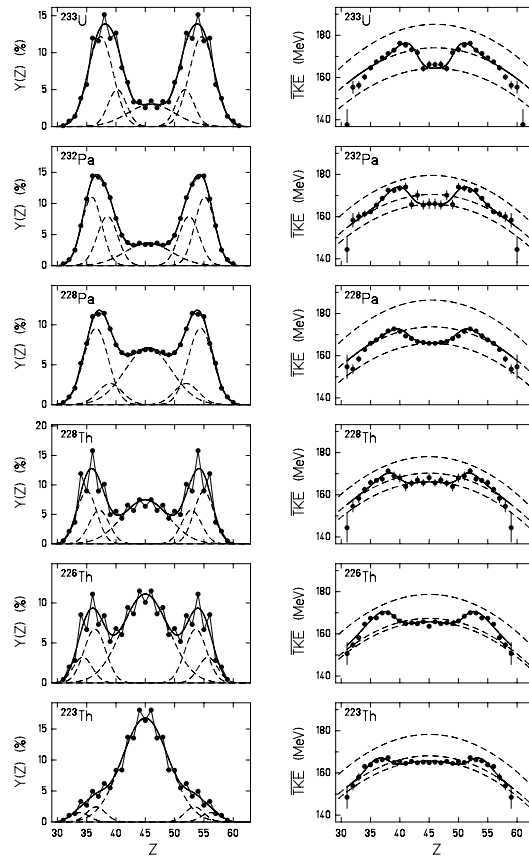The theoretical work on structure effects in fission presently concentrates

Figure 3. Element yields (left part) and average total kinetic energies (right part) as a function of the nuclear charge measured for fission fragments of several fissioning nuclei after electromagnetic excitations. The data points are compared to the result of a simultaneous fit (full lines) with 3 fission channels. The yields are defined as the sum, and the total kinetic energies are defined as the mean value of the individual contributions of the different channels. The super-long, standard I and standard II channels correspond to the symmetric, the inner asymmetric and the outer asymmetric peaks (dashed lines), respectively, in the yields and to the lower, upper and middle curve (dashed lines), respectively, in the total kinetic energies.

on the most realistic description of the shape-dependent potential-energy surface (e.g. Refs.[19,20]). The results look complicated, and the minimisation

with respect to higher-order shape distortions even introduces hidden discontinuities. These discontinuities make it even more difficult to perform full dynamical calculations in order to obtain quantitative predictions of the isotopic distributions of fission fragments. Up to now, these calculations rather serve as a guide to qualitatively relate the structures in the data to the structures in the potential-energy landscape.

Since theory cannot yet provide us with a quantitative prediction, we tried to understand the data with a semi-empirical approach. The basic idea of our approach has been inspired by considerations of Itkis *et al.*[21]. We consider the fission barrier under the condition of a certain mass asymmetry. The height of the fission barrier $V(A)$ is calculated as the sum of a liquid-drop barrier and two shells. The liquid-drop barrier is minimum at symmetry and grows quadratically as a function of mass asymmetry. The shell effects appear at $N = 82$ and $N \approx 90$. A more detailed description of the model is given in Ref.[22]. This picture provides us with an explanation for the predominance of asymmetric fission of the actinides. In ^{234}U like in most of the actinides, the lowest fission barrier appears for asymmetric mass splits. Approaching ^{264}Fm, the shell effects at $N = 82$ in both fragments join, giving rise to a narrow symmetric mass distribution. In lighter nuclei, the influence of these shells on the fission process is weakened, because they add up to the higher liquid-drop potential at larger mass asymmetry. In ^{208}Pb, the fission barrier is definitely lowest for symmetric mass splits.

A more quantitative description of this schematic model is given in Fig. 3. The mass yield $Y(A)$ is assumed to be proportional to the phase space $\rho(A)$ available above the fission barrier at a certain mass split. The initial excitation energy E^* above the mass-dependent barrier $V(A)$ is available for intrinsic excitations. The shell effect in the level density is washed out with energy as proposed by Ignatyuk *et al.*[23]. The stiffness of the underlying liquid-drop potential is deduced from a systematics of the width of measured mass distributions[24]. The shells are modelled in a way that the calculated yields $Y(Z)$ for ^{227}Th are reproduced.

Now the model is applied to other nuclei (^{224}Ac and ^{230}Pa) without any further adjustment. The shells move up and down on the liquid-drop potential just a little bit due to the shift in neutron number of the fissioning nucleus. These tiny variations are sufficient to substantially modify the shape of the element distribution just as much as the experimental distributions change. This good reproduction of the data is a strong argument that the global variations of the potential-energy surface as a function of the fissioning system give the correct explanation for the basic features of the transition from asymmetric to symmetric fission.
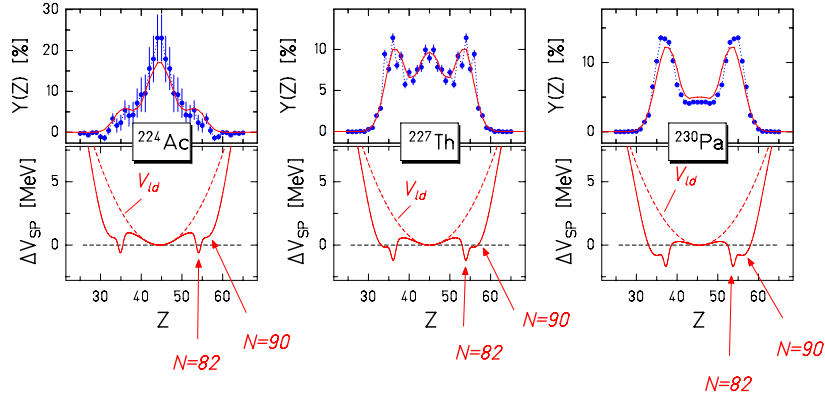
Figure 4. Measured element yields compared to the model predictions (upper parts), and the assumed variation ΔV of the fission barrier as a function of the nuclear charge of one fission fragment with respect to the fission barrier for symmetric splits (lower parts).

Figure 5 presents the element distributions, calculated with the same model, for all measured fissioning systems. There is an astonishingly good agreement with the experimental data for the whole systematics shown in Fig. 1. This success of the very simple model might indicate that the dynamics of the fission process tends to wash out the influence of the details of the potential-energy landscape. It is to be expected that due to the inertia of the collective motion the process does not feel every wiggle in the potential energy but rather takes a smooth trajectory.

Two specific features of the data, however, are not reproduced. Firstly, the ordering parameter of the calculated element distributions is not the mass but rather the neutron number. Secondly, the heavy fission component is not found to be constant at $Z = 54$ is as indicated in Fig. 2. This remarkable finding puts an important constraint on the theoretical description of the fission process. It may indicate that the shell effects in the proton subsystem play a more important role in asymmetric fission than currently assumed.

4   Summary

Nuclear fission is a unique laboratory due to a very specific feature which is not found in other systems: The electric charge in nuclei is homogeneously
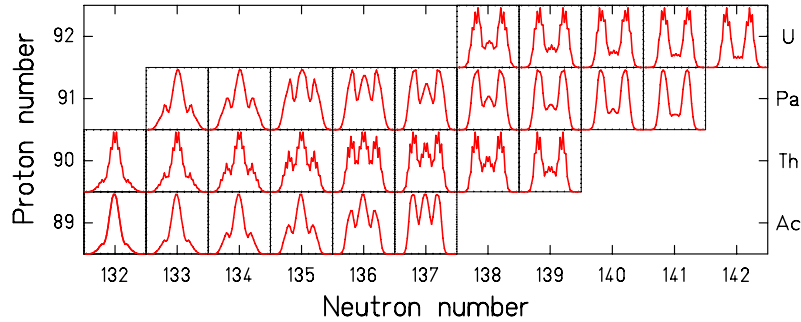
Figure 5. Calculated element distributions of fission fragments from electromagnetic-induced fission of 28 systems from ^{221}Ac to ^{234}U. See text for details.

distributed over the whole volume. This gives rise to a true fission process which is essentially symmetric. Shell effects in the order of a few MeV lead to very strong structural effects in the yields and in the kinetic energies of the fragments. Nuclear fission is thus a sensitive tool to investigate shell effects at large deformations.

Experiments with secondary beams using elaborate experimental installations available at GSI opened up new possibilities for experimental studies of nuclear fission. Element yields and total kinetic energies have been determined for 70 fissioning systems from ^{205}At to ^{234}U. In this way, new systematic results for a continuous region of fissioning systems have been obtained. The transition from symmetric to asymmetric fission has been traced back to the global features of the potential-energy landscape in the vicinity of the fission barrier. As a puzzling result the element distributions scale with the mass number of the fissioning system, and the heavy component of asymmetric fission is found to be centred at $Z = 54$ in all systems. In contrast to previous understanding, the data seem to indicate that shell effects in the proton subsystem play a major role in the fission process. Moreover, the super-long fission channel becomes more compact with decreasing mass of the fissioning system, demonstrating the influence of shell effects in symmetric mass splits, too.

References

1. R. Vandenbosch, J. R. Huizenga, *Nuclear Fission* (New York: Academic), 1973.
2. *The Nuclear Fission Process*, C. Wagemans, ed., CRC Press, London, 1991.
3. B. D. Wilkins, E. P. Steinberg, R. R. Chasman, *Phys. Rev.* C **14** (1976) 1832.
4. D. C. Hoffman, M. R. Lane, *Radiochimica Acta* **70/71** (1995) 135.
5. H. J. Specht, *Phys. Scripta* **10A** (1974) 21.
6. I. Nishinaka *et al.*, *Phys. Rev.* C **56** (1997) 891.
7. I. V. Pokrovsky *et al.*, *Phys. Rev.* C **60** (1999) 041304.
8. I. V. Pokrovsky *et al.*, *Phys. Rev.* C **62** (2000) 014615.
9. K.-H. Schmidt *et al.*, *Phys. Lett.* B **325** (1994) 313.
10. H.-G. Clerc *et al.*, *Nucl. Phys.* A **590** (1995) 785.
11. A. R. Junghans *et al.*, *Nucl. Phys.* A **629** (1998) 635.
12. K.-H. Schmidt *et al.*, *Nucl. Phys.* A **665** (2000) 221.
13. G. Baur, C. A. Bertulani, *Phys. Rev.* C **34** (1986) 1654.
14. K. F. Flynn *et al.*, *Phys. Rev.* C **5** (1972) 1725.
15. A. Turkevich, J. B. Niday, *Phys. Rev.* **84** (1951) 52.
16. V. V. Pashkevich, *Nucl. Phys.* A **169** (1971) 275.
17. M. G. Mustafa, U. Mosel, H. W. Schmitt, *Phys. Rev.* C **7** (1973) 1519.
18. U. Brosa, S. Grossmann, A. Mller, *Phys. Rep.* **197** (1990) 167.
19. V. V. Pashkevich, *Nucl. Phys.* A **477** (1988) 1.
20. P. Möller, A. Iwamoto, *Phys. Rev.* C **61** (2000) 047602.
21. M. G. Itkis *et al.*, *Sov. J. Part. Nucl.* **19** (1988) 301.
22. J. Benlliure *et al.*, *Nucl. Phys.* A **628** (1998) 458.
23. A. V. Ignatyuk, G. N. Smirenkin, A. S. Tiskin, *Yad. Fiz.* **21** (1975) 485 (*Sov. J. Nucl. Phys.* **21** (1975) 255).
24. S. I. Mulgin *et al.*, *Nucl. Phys.* A **640** (1998) 375.